

# Understanding Charge Transport in Molecular Electronics

J.G. KUSHMERICK,<sup>a</sup> S.K. POLLACK,<sup>a</sup> J.C. YANG,<sup>a</sup> J. NACIRI,<sup>a</sup>  
D.B. HOLT,<sup>a</sup> M.A. RATNER,<sup>b</sup> AND R. SHASHIDHAR<sup>a</sup>

<sup>a</sup>*Center for Bio/Molecular Science and Engineering,  
Naval Research Laboratory, Washington DC, USA*

<sup>b</sup>*Department of Chemistry, Northwestern University, Evanston, Illinois, USA*

**ABSTRACT:** For molecular electronics to become a viable technology the factors that control charge transport across a metal–molecule–metal junction need to be elucidated. We use an experimentally simple crossed-wire tunnel junction to interrogate how factors such as metal–molecule coupling, molecular structure, and the choice of metal electrode influence the current–voltage characteristics of a molecular junction.

**KEYWORDS:** molecular electronics; metal–molecule–metal junctions; tunnel junctions; charge transport

## INTRODUCTION

Studying charge transport across nanometer scale metal–molecule–metal junctions is an important step toward the realization of molecular-based electronics.<sup>1–4</sup> To this end a number of novel experimental approaches have been employed to measure charge transport across molecular junctions. These include scanning probe microscopies,<sup>5–14</sup> mechanical<sup>15–18</sup> and electromigration<sup>19,20</sup> break junctions, nanopores,<sup>21–24</sup> and mercury-drop electrodes.<sup>25,26</sup> To better understand charge transport in molecular electronic systems it would be beneficial to elucidate the role of different components within the junction. Conceptually a metal–molecule–metal junction can be partitioned into three discrete parts—the molecular core and the metal–molecule contacts on either side (see FIGURE 1). The chemical structure of the molecular core is amenable to a wide variety of possibilities; the majority of research has focused on aliphatic or aromatic systems, however, organometallic<sup>18–20,27</sup> and pseudo-rotaxane<sup>28–31</sup> systems have also been investigated. The nature of the two metal–molecule contacts is controlled by the choice of metal electrode as well as the chemical functionality or “alligator clip” that connects the molecule to the metal electrodes. The two metal–molecule contacts can be engineered to be the same or different by design of the molecule or electrode selection. Although the influences of the molecular core and metal–molecule contacts cannot be completely separated, we demonstrate in this paper that it can be instructive to investigate them independently.

Address for correspondence: J.G. Kushmerick, Center for Bio/Molecular Science and Engineering, Naval Research Laboratory, Washington, DC 20375, USA.  
kushmerick@nrl.navy.mil

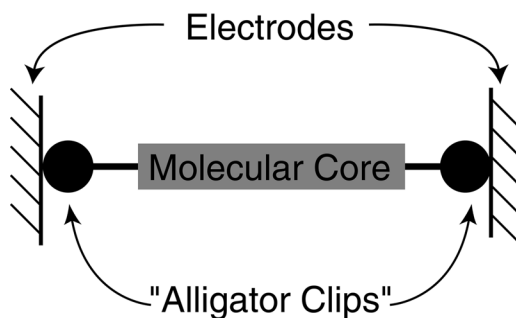


FIGURE 1. Schematic representation of a metal–molecule–metal junction.

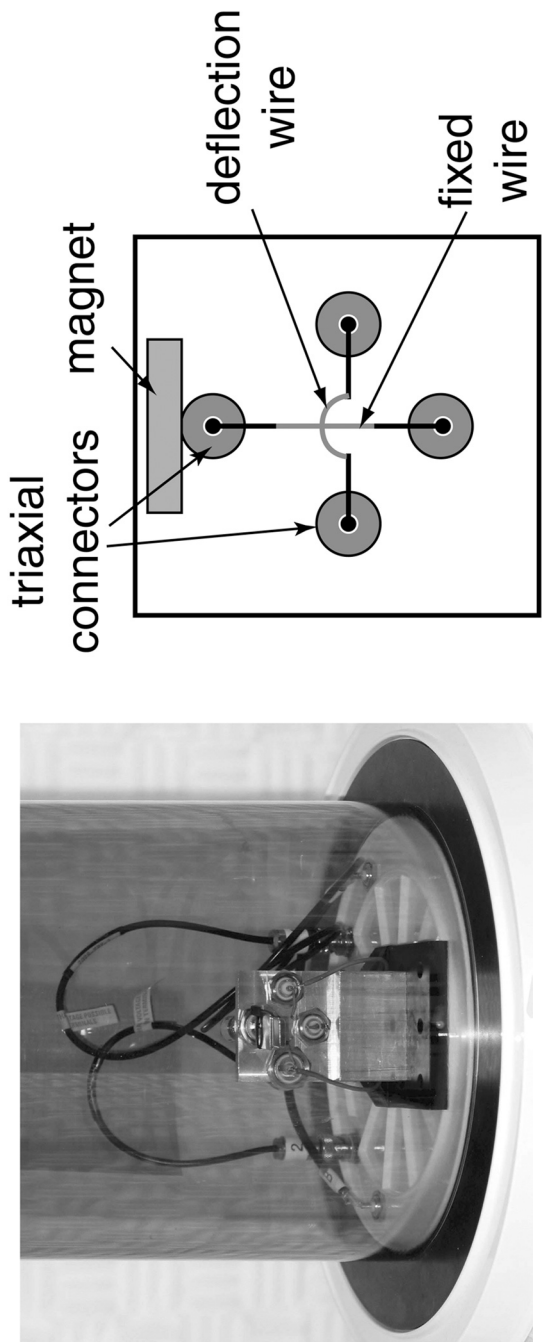
## EXPERIMENTAL DETAILS AND METHODS

### *I-V Characterization*

A photograph and schematic of the crossed-wire apparatus used in these experiments are shown in FIGURE 2. Two triaxial and two bnc bulkheads are mounted to an aluminum plate in a cross pattern. The 10- $\mu\text{m}$  diameter wires, one modified with a self-assembled monolayer of the molecule of interest, are mounted to the electrical connectors with indium solder. A rare earth magnet mounted onto the upper triaxial connector supplies a constant magnetic field (0.04 T at the junction) parallel to the fixed wire. The deflection wire is mounted so that it has a curved section perpendicular to the applied magnetic field and is about 1 mm from the fixed wire. The junction separation is controlled by bending the deflection wire with the Lorentz force generated from a small DC deflection current.<sup>34,35</sup> The deflection current is slowly increased, while monitoring the tunneling current at a fixed voltage of 0.5 V, to bring the wires gently together to form a junction at the contact point. After initial contact the junction “relaxes” over a time scale of several seconds to one minute to a stable conductance state. By comparison with other charge transport measurements, we calculate that junctions formed in this manner contain about  $10^3$  molecules.<sup>10,25</sup> The crossed-wire apparatus is housed in a nitrogen purged bell jar, which itself is inside a Faraday cage. Current–voltage characteristics of the molecular junctions were recorded by an Agilent 4155B semiconductor parameter analyzer via the two triaxial connectors. All measurements were made at room temperature.


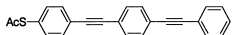
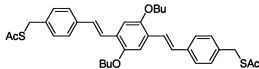
### *Molecular Self-Assembly*

A list of the compounds used in this study as well as some of their important physical parameters is given in TABLE 1. Self-assembled monolayers for *I-V* measurements were prepared on 10- $\mu\text{m}$  diameter Au wires (Goodfellow, Berwyn, Pennsylvania). The gold wires were cleaned in 30%  $\text{H}_2\text{O}_2$  followed by a rinse in  $\text{H}_2\text{O}$  and ethanol. SAMs were deposited from 1-mM solutions in a 50/50 mixture of ethanol/tetrahydrofuran. Monolayers were formed directly from the thioacetates to avoid the formation of multilayers through disulfide linkages.<sup>36</sup> Monolayers formed



**FIGURE 2.** Photograph and schematic of the crossed-wire tunnel junction. See text for full experimental details.

TABLE 1. List of compounds used

Compound	Molecular Structure	Molecular Length (Å) <sup>a</sup>	$E_g$ (eV) <sup>b</sup>
1	AcS(CH <sub>2</sub> ) <sub>12</sub> SAc	14.6	7.11
2	HS(CH <sub>2</sub> ) <sub>11</sub> CH <sub>3</sub>	13.4	7.16
3		20.2	3.51
4		19.5	3.60
5		20.5	3.12

<sup>a</sup>Molecular length is defined as the sulfur to sulfur distance for compounds **1**, **3**, and **5** and the sulfur to terminal hydrogen distance for compounds **2** and **4**.

<sup>b</sup> $E_g$  is the calculated HOMO–LUMO gap.

Both molecular length and  $E_g$  are determined from optimized structures at the B3LYP/6-31G\* level of density functional theory.

on flat Au substrates under the same deposition conditions yielded well-packed monolayers, as determined by spectroscopic ellipsometry and water contact angle measurements.

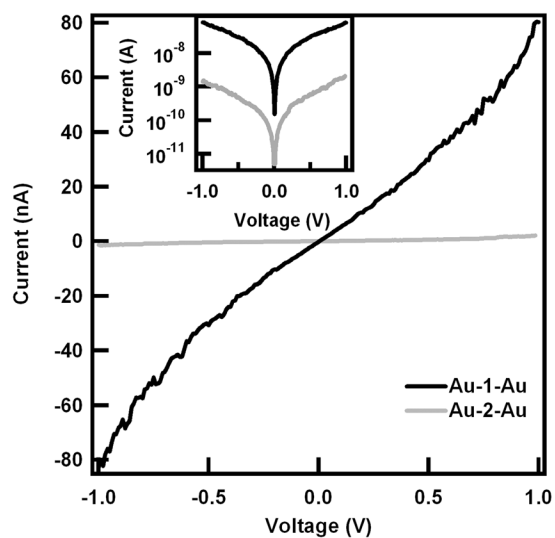
## RESULTS AND DISCUSSION

### Role of Metal–Molecule Contacts

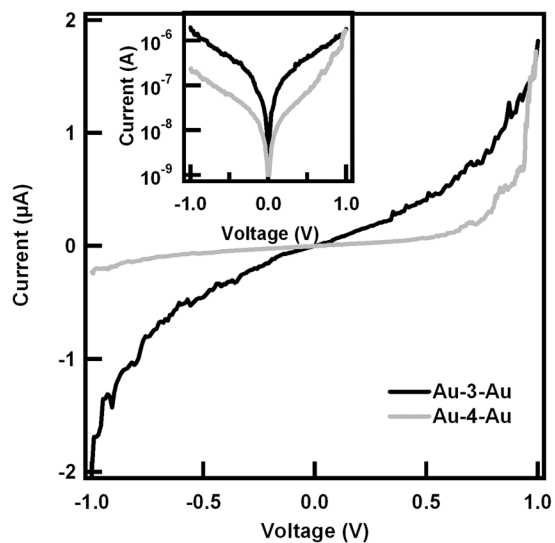
To explore the effect of the metal–molecule contacts on the  $I$ – $V$  characteristics, two classes of molecules—insulating alkyl molecules (**1** and **2**) and rigid  $\pi$ -conjugated molecules based on oligo(phenylene ethynylene) (OPE) (**3** and **4**)—with mono- and  $\alpha,\omega$ -dithio functionalities were investigated. Junctions formed from the monothio species yield molecular junctions that are inherently asymmetric due to the different metal–molecule contacts—a strong thiolate linkage at one interface and a weak *mechanical* linkage at the other.

FIGURE 3 shows the  $I$ – $V$  characteristics for junctions containing alkyl monolayers of **1** and **2** between two gold wires. Both junctions produce very symmetric  $I$ – $V$  characteristics (FIG. 3) but the conductance of the dithiolate dodecane junction is more than an order of magnitude higher than that of the monothiolate. Higher electron transport through alkane chains chemically bound (through thiolate linkages) to Au electrodes at both ends than those bonded only at one electrode was recently reported for scanning probe measurements on small bundles of molecules.<sup>11</sup> The chemical bond between molecule and electrode provides a connection between the molecular electronic structure with the band structure of the metal. Thus, it is not surprising that a stronger connection leads to an enhancement in charge transport efficiency.

A junction formed from a monolayer of the dithioacetate OPE molecule **3** also exhibits symmetric  $I$ – $V$  characteristics with respect to bias polarity—as would be expected for a symmetric junction (see FIGURE 4). Analogous to the alkane molecules, the conductivity of a junction formed from **3** is roughly an order of magnitude



**FIGURE 3.**  $I$ - $V$  characteristics of alkane junctions. The dithioacetyl alkane Au-1-Au is more than an order of magnitude more conductive than the monothioacetyl Au-2-Au.

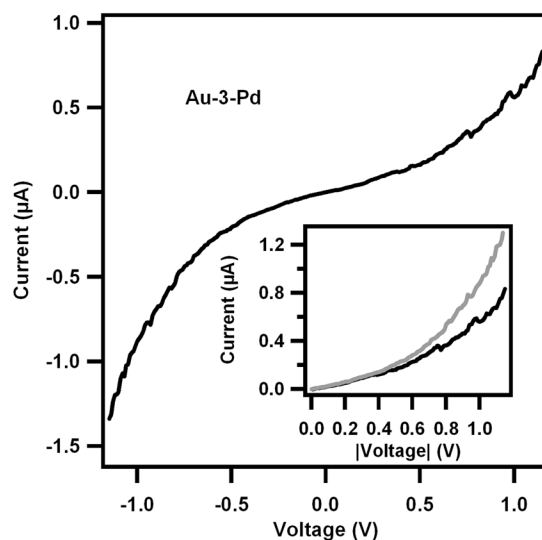


**FIGURE 4.**  $I$ - $V$  characteristics of Au-3-Au and Au-4-Au junctions. The large asymmetry seen in the Au-4-Au junction results from the different metal-molecule contacts on either side of the junction. The positive branch of the  $I$ - $V$  trace corresponds to electron injection at the Au-phenylene interface.

higher than that from a junction of **4** over the entire bias (inset of FIG. 4). Compared to the alkyl system, an asymmetric metal–molecule contact has a large effect on the  $I$ – $V$  characteristics symmetry. The  $I$ – $V$  characteristics of a junction formed from the asymmetric OPE **4** exhibits a prominent rectification behavior (FIG. 4) above an onset near 0.7 V, with the current at +1 V more than seven times larger than that at –1 V. Forward bias corresponds to electrons injected at the Au–phenylene interface. Other instances of  $I$ – $V$  asymmetries arising from differences in metal–molecule contacts or coupling have been reported. Rectification has also been previously reported for molecular junctions with nonequivalent metal–molecule contacts. Reed and coworkers observed large rectification for a biphenylthiolate monolayer in a nanopore.<sup>21</sup> Sita and coworkers also reported rectification from scanning tunneling spectroscopy measurements of **4**<sup>37</sup> and Weber and coworkers demonstrated that a molecule with nominally symmetric metal–molecule contacts can yield asymmetric  $I$ – $V$  characteristics when one of the metal–molecule bonds is distorted in a mechanically controlled break junction.<sup>17</sup>

Theoretical calculations have shown that asymmetric  $I$ – $V$  characteristics can result from differences in coupling at the two metal–molecule contacts which leads to different voltage drops and injection barriers at the two interfaces.<sup>32,38–41</sup> In our case the electronic coupling afforded by the Au–S contact pins the molecular levels of **4** relative to the Fermi level of that Au electrode. The major voltage drop occurs at the Au–phenylene interface.<sup>42</sup> Considering the bias polarity and the voltage drop, it is most likely that electrons injected at the Au–phenylene interface start to couple strongly to an unoccupied frontier orbital of the extended molecule electrode system. Although the dominant transport at voltages greater than +0.5 V for monothioacetyl OPE is likely the result of electron tunneling, the low bias conduction (which is very symmetric) is likely due to hole tunneling. The onset of resonance with an unoccupied molecular orbital opens up another conduction channel for this system, resulting in the large rectification. The fact that the monothiolate alkane junction does not exhibit a stronger bias asymmetry is an indication of the molecules large HOMO–LUMO gap (TABLE 1). Over the limited bias voltage range investigated here, we are far from molecular resonances and, thus, the efficiency of charge transport is only minimally influenced by the bias polarity.

The choice of electrode metal affects both the nature of the metal–molecule bond and the electronic coupling since the work function and metal–molecule bonding are both modified. Previous measurements of charge transport across alkyl monolayers suggest a correlation between the work function of a metal and the contact resistance (junction resistance extrapolated to zero chain length).<sup>13</sup> Metals with higher work functions exhibited lower contact resistances, which was attributed to better hole injection due to enhanced coupling to the highest occupied molecular orbital (HOMO). Recent theoretical calculations based on a  $\pi$ -conjugated *molecular wire* suggested that a good chemical linkage group (often referred to as *alligator clip*)–metal combination for facilitating charge transport is S–Pd, whereas the S–Au combination is one of the worst.<sup>43</sup> To experimentally address this prediction, we measured the transport properties of a junction formed from a monolayer of **3** between a Au and Pd wire (see FIGURE 5). There is a distinct asymmetry in the  $I$ – $V$  characteristics, although the relative difference is small (1.5 times more current at –1 V than at +1 V). *Ab initio* calculations for this system (not shown) suggest that charge transport

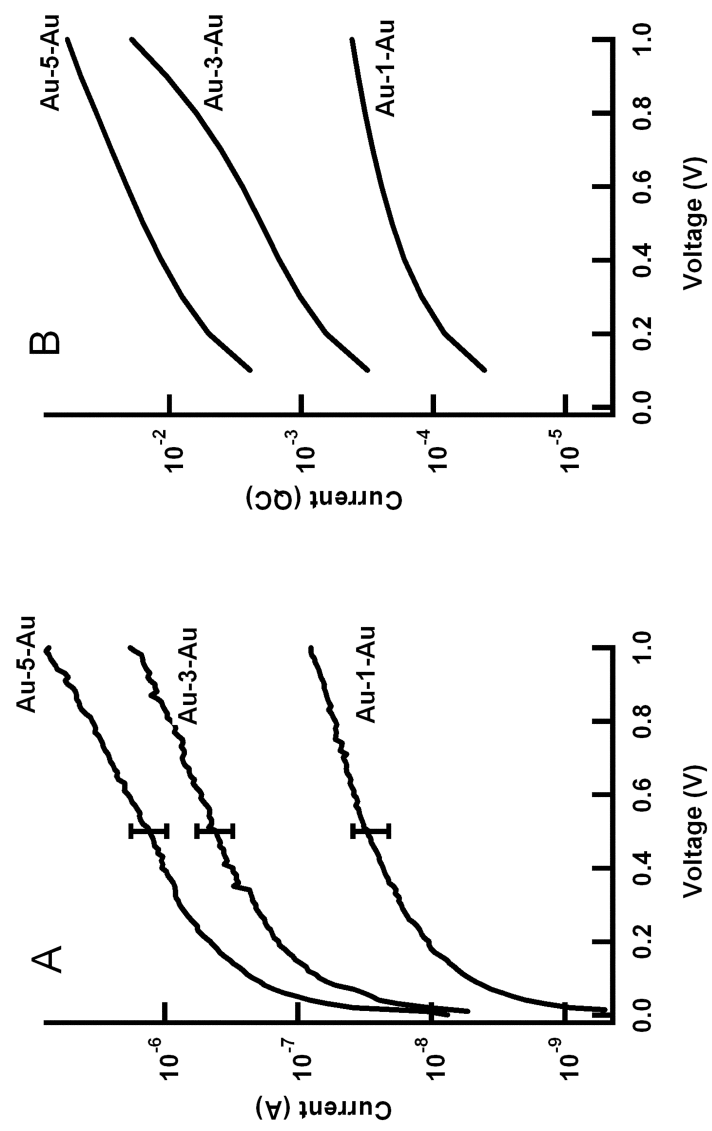


**FIGURE 5.**  $I$ - $V$  characteristics of a Au-3-Pd junction. The higher conductivity of the negative branch of the  $I$ - $V$  trace corresponds to hole injection at the Pd-thiolate interface. The **inset** highlights the bias polarity asymmetry by plotting the current versus the absolute value of bias voltage.

proceeds through coupling to the HOMO level (hole conduction) since its delocalized nature is more suited to act as a conduction channel than the LUMO, which is isolated at the Au-S interface. The measured  $I$ - $V$  characteristics can, thus, be understood by the fact that the Pd-S interface exhibits a smaller barrier for hole injection than that of the Au-S interface. In fact, calculations have predicted that the Pd-S interface is an almost barrierless contact.<sup>43</sup> The Au-S interface and the transport through the molecular core limit the overall conductance of the system.

#### *Effect of Molecular Structure on Charge Transport*

Although a number of experiments on molecular junctions have looked directly at charge transport as a function of molecular structure,<sup>5,8,10,12,25,26</sup> there is also a large body of knowledge from electrochemical<sup>44-47</sup> and donor-bridge-acceptor<sup>48-51</sup> measurements of electron-transfer rates. Two particular classes of molecular wires, oligo(phenylene ethynylene) (OPE) and oligo(phenylene vinylene) (OPV), have been the focus of much study. It has previously been argued that the higher planarity of OPV makes it a better molecular wire than OPE, however, the measurements and theoretical calculations presented here highlight a second important contribution to molecular wire conductance: the extent of bond-length alternation along the  $\pi$ -conjugated molecular backbone. FIGURE 6A shows the experimental  $I$ - $V$  characteristics for junctions containing alkane **1**, oligo(phenylene ethynylene) **3**, and oligo(phenylene vinylene) **5** molecules. The error bars associated with the measurements are attributed to variations in junction area between independent junctions.



**FIGURE 6.** Experimental (A) and theoretical (B) plots of current (logarithmic scale) as a function of the applied bias voltage for junctions formed from the three compounds studied. The theoretical traces are given in units of the quantum of current ( $2e^2/h$  volt).



Multiple measurements on the same junction show a much smaller deviation. As would be expected, there is a clear difference in the efficiency of charge transport across monolayers between the electrically-insulating  $\sigma$ -bonded alkane and that of the  $\pi$ -conjugated oligo(phenylene ethynylene) (OPE) and oligo(phenylene vinylene) (OPV) molecular wires. The difference in conductance between OPE and OPV is discussed below.

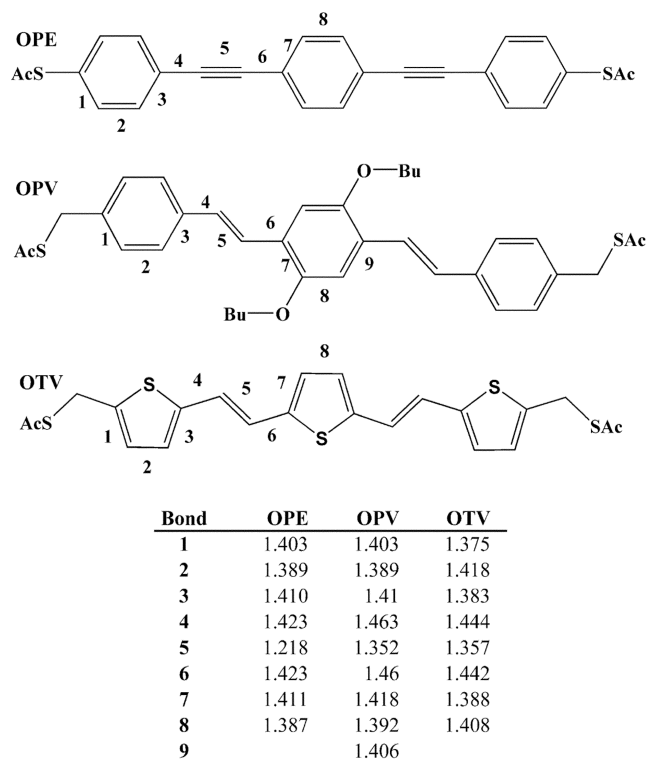
To better understand the physical basis for the measured  $I$ - $V$  characteristics,  $I$ - $V$  traces were calculated using extended Huckel theory (EHT) and Green's function (GF) techniques under the approximation that the entire potential drop occurs at the metal-molecule interfaces. Since only low bias ranges ( $\pm 1$  V) were considered, charging effects were neglected. These theoretical methods have been outlined in detail by Ratner<sup>54</sup> and Datta.<sup>38,40</sup> The simplest possible model systems were used, that is, single metal atoms contacting the molecular species. The EHT/GF treatment allows the calculation of the transmission function,  $T(E, V)$ , which is then used in the standard scattering equation from mesoscale physics to calculate the  $I$ - $V$  characteristics<sup>55</sup>

$$I = \frac{2e}{h} \int_{-\infty}^{\infty} T(E, V) [f(E - \mu_2) - f(E - \mu_1)] dE, \quad (1)$$

where  $\mu_1 = E_f - \eta eV$ ,  $\mu_2 = E_f + (1 - \eta)eV$ , and  $f(E - \mu_i)$  are the Fermi distributions for the two contacts referenced to their electrochemical potentials ( $\mu_i$ ), which are functions of the equilibrium Fermi level ( $E_f$ ) and the voltage division factor ( $\eta$ ). The latter describes how the total potential drop ( $V$ ) is separated between the two metal-molecule interfaces.<sup>38</sup> Since all three junctions in this study have symmetric metal-molecule attachments we assume that the voltage drop is split equally at both interfaces ( $\eta = 0.5$ ).

The calculated  $I$ - $V$  characteristics are in excellent qualitative agreement with the experimental measurements (FIG. 6B). Both experiment and theory show the same trend in molecular conductance, namely **1** < **3** < **5**. This ordering of charge transport efficiency is consistent with electrochemical measurements on related systems.<sup>44-47</sup> Now we turn our attention to the differences in charge transport for OPE and OPV. It has previously been argued that the higher coplanarity and, thus, better  $\pi$ -conjugation of OPV systems compared to that of OPE (in which the phenylene rings are freely rotating at room temperature) explains the more facile charge transport in OPV.<sup>45,47,56,57</sup> Charge transport calculations as a function of coplanarity demonstrate that conductance is reduced when the phenyl rings of a conjugated system are rotated with respect to each other.<sup>58,59</sup> Notwithstanding the effect of coplanarity, our calculations indicate a second important factor that impacts a molecules conductance. Since the transport calculations reported in FIGURE 6B were performed for single molecules rigidly fixed at their energy minimized structures (approximately planar for both molecules), the differences in calculated conductance cannot be attributed to disruption of  $\pi$ -conjugation due to phenylene ring rotation. Therefore, we argue that the higher conductivity is a result of the smaller bond-length alternation in OPV compared to that in OPE.

If we consider the molecules as one-dimensional crystals (see FIGURE 7), we see that the short (1.218 Å) ethynylene linkage in OPE disrupts the periodicity of the  $\pi$ -conjugated molecular backbone ( $1.41 \pm 0.01$  Å) more drastically than the vinylene linkage in OPV (1.352 Å, backbone,  $1.41 \pm 0.03$  Å). From studies of conducting



**FIGURE 7.** Bond lengths (reported in Å) of the conjugated backbone for molecules **3**, **5**, and oligo(thiophene vinylene) OTV, a proposed molecular wire.

polymers we know that the size of the HOMO–LUMO gap is directly related to the extent of bond-length alternation.<sup>60,61</sup> The greater bond-length alternation in OPE, thus, causes it to have a larger HOMO–LUMO gap than OPV, as shown in TABLE 1. At low applied bias, transport is dominated by charge carrier tunneling inside the HOMO–LUMO gap (non-resonant tunneling). The difference in energy between the Au Fermi level and the closest molecular orbital (HOMO or LUMO) defines the tunneling barrier for the system. The smaller HOMO–LUMO gap of OPV leads to a smaller tunneling barrier and a higher conductance. In the language of solid state physics, OPV can be thought of as having a smaller Peierls distortion than OPE and, thus, acts more like a one-dimensional metal.<sup>62</sup> Analyzing molecular conductance in terms of bond length alternation should enable molecular wires with better transport properties to be predicted and subsequently synthesized and measured. For example the oligo(thiophene vinylene) (OTV) molecule shown schematically in FIGURE 7 has an even lower degree of bond-length alternation (vinylene linkage, 1.357 Å; molecular backbone, 1.40 ± 0.03 Å) and is predicted to have a HOMO–LUMO gap of 2.77 eV.

It is important to note that the methylene groups between the thioacetyl and phenylene ring on either end of the OPV molecule (and the gedanken molecule OTV) undoubtedly act as barriers to charge transport (and as local sources of charge build-up and voltage drop). We estimate that the presence of these two methylene groups reduces the junction conductance by a factor of three to eight.<sup>25</sup> We are currently investigating the properties of a related OPV molecule without methylene spacers to directly determine their effect.

## CONCLUSIONS AND FUTURE DIRECTIONS

We report initial studies of charge transport across organic molecules in an attempt to understand how the various components of a metal–molecule–metal junction affect the  $I$ – $V$  characteristics. We have shown (1) that differences in metal–molecule contacts can lead to asymmetric  $I$ – $V$  characteristics, (2) that poor electrode–molecule coupling due to the lack of a chemical bond can inhibit charge transfer, and (3) that the extent of bond-length alternation needs to be considered to fully understand charge transport across  $\pi$ -conjugated molecular wires. Although we feel these studies point out some of the important factors in charge transport across molecular junctions, additional studies that include other alligator clip/metal combinations, as well as other molecular structures, are needed to fully map out the relevant interactions.  $I$ – $V$  characteristics as a function of temperature are critical to completely understand the conduction mechanism(s) (including the transition to incoherent transport) in molecular electronic systems. Such studies are currently in progress.

## ACKNOWLEDGMENTS

Financial support of the Defense Advanced Research Projects Agency (DARPA) Moletronics program is gratefully acknowledged. One of us (J.C.Y.) is thankful to the National Research Council.

## REFERENCES

1. AVIRAM, A. & M.A. RATNER. 1974. Molecular rectifiers. *Chem. Phys. Lett.* **29**: 277–283.
2. JOACHIM, C., J.K. GIMZEWSKI & A. AVIRAM. 2000. Electronics using hybrid-molecular and mono-molecular devices. *Nature* **408**: 541–548.
3. RATNER, M.A. 2002. Introducing molecular electronics. *Mater. Today* **5**: 20–27.
4. KWOK, K.S. & J.C. ELLENBOGEN. 2002. Moletronics: future electronics. *Mater. Today* **5**: 28–37.
5. BUMM, L.A., *et al.* 1996. Are single molecular wires conducting? *Science* **271**: 1705–1707.
6. ANDRES, R.P., *et al.* 1996. “Coulomb staircase” at room temperature in a self-assembled molecular nanostructure. *Science* **272**: 1323–1325.
7. WEISS, P.S., *et al.* 1998. Probing electronic properties of conjugated and saturated molecules in self-assembled monolayers. *Ann. N.Y. Acad. Sci.* **852**: 145–168.
8. CYGAN, M.T., *et al.* 1998. Insertion; conductivity; and structures of conjugated organic oligomers in self-assembled alkanethiol monolayers on Au{111}. *J. Am. Chem. Soc.* **120**: 2721–2732.
9. DONHAUSER, Z.J., *et al.* 2001. Conductance switching in single molecules through conformational changes. *Science* **292**: 2303–2307.

10. WOLD, D.J. & C.D. FRISBIE. 2001. Fabrication and characterization of metal–molecule–metal junctions by conducting probe atomic force microscopy. *J. Am. Chem. Soc.* **123**: 5549–5556.
11. CUI, X.D., *et al.* 2001. Reproducible measurement of single-molecule conductivity. *Science* **294**: 571–574.
12. WOLD, D.J., *et al.* 2002. Distance dependence of electron tunneling through self-assembled monolayers measured by conducting probe atomic force microscopy: unsaturated versus saturated molecular junctions. *J. Phys. Chem. B* **106**: 2813–2816.
13. BEEBE, J.M., *et al.* 2002. Contact resistance in metal–molecule–metal junctions based on aliphatic SAMs: effects of surface linker and metal work function. *J. Am. Chem. Soc.* **124**: 11268–11269.
14. SZUCHMACHER BLUM, A., *et al.* 2003. Comparing the conductivity of molecular wires with the scanning tunneling microscope. *Appl. Phys. Lett.* **82**: 3322–3324.
15. REED, M.A., *et al.* 1997. Conductance of a molecular junction. *Science* **278**: 252–254.
16. KERGUERIS, C., *et al.* 1999. Electron transport through a metal–molecule–metal junction. *Phys. Rev. B* **59**: 12505–12513.
17. REICHERT, J., *et al.* 2002. Driving current through single molecules. *Phys. Rev. Lett.* **88**: 176804–176807.
18. MAYOR, M., *et al.* 2002. A trans-platinum(II) complex as a single-molecule insulator. *Angew. Chem. Intl. Edn.* **41**: 1183–1186.
19. PARK, J., *et al.* 2002. Coulomb blockade and the Kondo effect in single-atom transistors. *Nature* **417**: 722–725.
20. LIANG, W., *et al.* 2002. Kondo resonance in a single-molecule transistor. *Nature* **417**: 725–729.
21. ZHOU, C., *et al.* 1997. Nanoscale metal/self-assembled monolayer/metal heterostructures. *Appl. Phys. Lett.* **71**: 611–613.
22. CHEN, J., *et al.* 1999. Large on–off ratios and negative differential resistance in a molecular electronic device. *Science* **286**: 1550–1552.
23. CHEN, J., *et al.* 1999. Electronic transport through metal-1,4-phenylene diisocyanide-metal junctions. *Chem. Phys. Lett.* **313**: 741–748.
24. REED, M.A., *et al.* 2001. Molecular random access memory cell. *Appl. Phys. Lett.* **78**: 3735–3737.
25. HOLMLIN, R.E., *et al.* 2001. Electron transport through thin organic films in metal–insulator–metal junctions based on self-assembled monolayers. *J. Am. Chem. Soc.* **123**: 5075–5085.
26. HOLMLIN, R.E., *et al.* 2001. Correlating electron transport and molecular structure in organic thin films. *Angew. Chem. Intl. Edn.* **40**: 2316–2320.
27. SCHULL, T.L., *et al.* 2003. Ligand effects on charge transport in platinum(II) acetylides. *J. Am. Chem. Soc.* **125**: 3202–3203.
28. COLLIER, C.P., *et al.* 1999. Electronically configurable molecular-based logic gates. *Science* **285**: 391–394.
29. COLLIER, C.P., *et al.* 2000. A [2]catenane-based solid state electronically reconfigurable switch. *Science* **289**: 1172–1175.
30. COLLIER, C.P., *et al.* 2001. Molecular-based electronically switchable tunnel junction devices. *J. Am. Chem. Soc.* **123**: 12632–12641.
31. LUO, Y., *et al.* 2002. Two-dimensional molecular electronics circuits. *Chem. Phys. Chem.* **3**: 519–525.
32. KUSHMERICK, J.G., *et al.* 2002. Metal-molecule contacts and charge transport across monomolecular layers: measurement and theory. *Phys. Rev. Lett.* **89**: 086802.
33. KUSHMERICK, J.G., *et al.* 2002. Effect of bond-length alternation in molecular wires. *J. Am. Chem. Soc.* **124**: 10654–10655.
34. GREGORY, S. 1990. Inelastic tunneling spectroscopy and single-electron tunneling in an adjustable microscopic tunnel junction. *Phys. Rev. Lett.* **64**: 689–692.
35. ZIMMERMAN, D.T. & G. AGNOLET. 2001. Inelastic electron tunneling spectroscopy measurements using adjustable oxide-free tunnel junctions. *Rev. Sci. Instrum.* **72**: 1781–1787.

36. TOUR, J.M., *et al.* 1995. Self-assembled monolayers and multilayers of conjugated thiols, alpha omega-dithiols, and thioacetyl-containing adsorbates. Understanding attachments between potential molecular wires and gold surfaces. *J. Am. Chem. Soc.* **117**: 9529–9534.
37. DHIRANI, A.-A., *et al.* 1997. Self-assembled molecular rectifiers. *J. Chem. Phys.* **106**: 5249–5253.
38. DATTA, S., *et al.* 1997. Current–voltage characteristics of self-assembled monolayers by scanning tunneling microscopy. *Phys. Rev. Lett.* **79**: 2530–2533.
39. TIAN, W., *et al.* 1998. Conductance spectra of molecular wires. *J. Chem. Phys.* **109**: 2874–2882.
40. HONG, S., *et al.* 2000. Molecular conductance spectroscopy of conjugated, phenyl-based molecules on Au(111): the effect of end groups on molecular conduction. *Superlat. Microstruct.* **28**: 289–303.
41. TAYLOR, J., M. BRANDBYGE & K. STOKBRO. 2002. Theory of rectification in Tour wires: the role of electrode coupling. *Phys. Rev. Lett.* **89**: 138301.
42. GONZALEZ, C., V. MUJICA & M.A. RATNER. 2002. Modeling of electrostatic potential spatial profile of molecular junctions: the influence of defects and weak links. *Ann. N.Y. Acad. Sci.* **960**: 163–176.
43. SEMINARIO, J.M., C.E. DE LA CRUZ & P.A. DEROSA. 2001. A theoretical analysis of metal–molecule contacts. *J. Am. Chem. Soc.* **123**: 5616–5617.
44. CHIDSEY, C.E.D. 1991. Free energy and temperature dependence of electron transfer at the metal–electrolyte interface. *Science* **251**: 919–922.
45. SACHS, S.B., *et al.* 1997. Rates of interfacial electron transfer through  $\pi$ -conjugated spacers. *J. Am. Chem. Soc.* **119**: 10563–10564.
46. WEBER, K., L. HOCKETT & S. CREAGER. 1997. Long-range electronic coupling between ferrocene and gold in alkanethiolate-based monolayers on electrodes. *J. Phys. Chem. B* **101**: 8286–8291.
47. CREAGER, S., *et al.* 1999. Electron transfer at electrodes through conjugated “molecular wire” bridges. *J. Am. Chem. Soc.* **121**: 1059–1064.
48. CLOSS, G.L. & J.R. MILLER. 1988. Intramolecular long-distance electron transfer in organic molecules. *Science* **240**: 440–447.
49. FOX, L.S., *et al.* 1990. Gaussian free-energy dependence of electron-transfer rates in iridium complexes. *Science* **247**: 1069–1071.
50. HELMS, A., D. HEILER & G. MCLENDON. 1992. Electron transfer in *bis*-porphyrin donor–acceptor compounds with polyphenylene spacers shows a weak distance dependence. *J. Am. Chem. Soc.* **114**: 6227–6238.
51. DAVIS, W.B., *et al.* 1998. Molecular-wire behaviour in *p*-phenylenevinylene oligomers. *Nature* **396**: 60–63.
52. MARDER, S.R., *et al.* 1997. Design and synthesis of chromophores and polymers for electro-optic and photorefractive applications. *Nature* **388**: 845–851.
53. OLSON, M., *et al.* 1998. A conformational study of the influence of vibrations on conduction in molecular wires. *J. Phys. Chem. B* **102**: 941–947.
54. MUJICA, V., M. KEMP & M.A. RATNER. 1994. Electron conduction in molecular wires. I. A scattering formalism. *J. Chem. Phys.* **101**: 6849–6855.
55. DATTA, S. 1995. *Electronic Transport in Mesoscopic Systems*. Cambridge University Press, Cambridge.
56. SIKES, H.D., *et al.* 2001. Rapid electron tunneling through oligophenylenevinylene bridges. *Science* **291**: 1519–1523.
57. DUDEK, S.P., H.D. SIKES & C.E.D. CHIDSEY. 2001. Synthesis of ferrocenethiols containing olig(phenylenevinylene) bridges and their characterization on gold electrodes. *J. Am. Chem. Soc.* **123**: 8033–8038.
58. SAMANTA, M.P., *et al.* 1996. Electronic conduction through organic molecules. *Phys. Rev. B* **53**: R7626–R7629.
59. SEMINARIO, J.M. & P.A. DEROSA. 2001. Molecular gain in a thiotolane system. *J. Am. Chem. Soc.* **123**: 12418–12419.
60. HEEGER, A.J. 2001. Semiconducting and metallic polymers: the fourth generation of polymeric materials. *J. Phys. Chem. B* **105**: 8475–8491.

61. FARCHIONI, R. & G. GROSSO. 2001. Organic electronic materials: conjugated polymers and low molecular weight organic solids. *Mater. Sci.* **41**: 448.
62. PEIERLS, R.E. 1955. *Quantum Theory of Solids*. Oxford University Press, London.